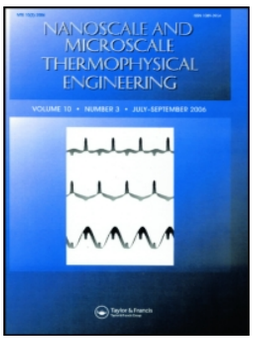

Nanoscale and Microscale Thermophysical Engineering

ISSN: 1556-7265 (Print) 1556-7273 (Online) Journal homepage: http://www.tandfonline.com/loi/umte20

First Principles Peierls-Boltzmann Phonon Thermal Transport: A Topical Review

Lucas Lindsay

To cite this article: Lucas Lindsay (2016) First Principles Peierls-Boltzmann Phonon Thermal Transport: A Topical Review, Nanoscale and Microscale Thermophysical Engineering, 20:2, 67-84, DOI: 10.1080/15567265.2016.1218576

To link to this article: http://dx.doi.org/10.1080/15567265.2016.1218576

Accepted author version posted online: 05 Aug 2016.
Published online: 05 Aug 2016.

NANOSCALE AND MICROSCALE THERMOPHYSICAL ENGINEERING
2016, VOL. 20, NO. 2, 67–84
http://dx.doi.org/10.1080/15567265.2016.1218576

Taylor & Francis
Taylor & Francis Group

First Principles Peierls-Boltzmann Phonon Thermal Transport: A Topical Review

Lucas Lindsay

Materials Science and Technology Division, Oak Ridge National Laboratory, Oak Ridge, Tennessee, USA

ABSTRACT

The advent of coupled thermal transport calculations with interatomic forces derived from density functional theory has ushered in a new era of fundamental microscopic insight into lattice thermal conductivity. Subsequently, significant new understanding of phonon transport behavior has been developed with these methods, and because they are parameter free and successfully benchmarked against a variety of systems, they also provide reliable predictions of thermal transport in systems for which little is known. This topical review will describe the foundation from which first principles Peierls-Boltzmann transport equation methods have been developed and briefly describe important necessary ingredients for accurate calculations. Sample highlights of reported work will be presented to illustrate the capabilities and challenges of these techniques and to demonstrate the suite of tools available, with an emphasis on thermal transport in micro- and nanoscale systems. Finally, future challenges and opportunities will be discussed, drawing attention to prospects for methods development and applications.

ARTICLE HISTORY
Received June 18, 2016
Accepted July 26, 2016

KEYWORDS
Thermal transport; photon scattering; first principles; density functional theory

Introduction

In light of our changing world (interwoven globalization of politics, economics, climate perspectives), a considerable focus of recent fundamental research and basic engineering applications is energy efficiency. One broad pillar of such scientific and technological pursuits is built from fundamental understanding of thermophysical processes, of heat and ways to manipulate it in our environment and in materials. Significant strides have been taken to increase thermal efficiency on many scales from industrial applications and combustion engines [1] to nanoscale thermal energy storage and transfer [2, 3]. Some thermophysical engineering drivers promoting recent thermal transport research include high-efficiency thermoelectric materials for waste heat capture and solid-state refrigeration [4], thermal barrier coatings in combustion turbines [5], and thermal interface and heat dissipation materials in electronics packaging [6]. A fundamental physical property that plays a critical role in determining the utility of a material for such applications is thermal conductivity or, for the main discussion in this topical review, lattice thermal conductivity, κ. Among the more fundamental and important recent advances in thermal transport is the advent of predictive first principles calculations of κ, determination of κ without adjustable parameters [7, 8] (see Figure 1).

CONTACT Lucas Lindsay lindsaylr@ornl.gov Oak Ridge National Laboratory, Materials Science and Technology Division, PO Box 2008 MS 6056, Oak Ridge, TN 37831.

Color versions of one or more of the figures in the article can be found online at www.tandfonline.com/umte.

Nomenclature

a	acoustic or lattice constant, Å
a–o	frequency gap between acoustic and optic branches
C	volume normalized specific heat, $JK^{-1}m^{-3}$
D	dynamical matrix, $Jm^{-2}kg^{-1}$
fp-PBT	first principles Peierls-Boltzmann transport equation
G	reciprocal lattice vector, $Å^{-1}$
j	branch index
m	mass, kg
N	normal
n	nonequilibrium distribution
o	optic
q	wavevector, $Å^{-1}$
R	lattice vector, Å
T	temperature, K
U	Umklapp
v	velocity, m/s
V	volume, m^3, or crystal potential, J
Z	thermoelectric figure of merit, K^{-1}
ZA	out-of-plane flexural acoustic
2D	two dimensional
Greek Symbols	
κ	lattice thermal conductivity, $Wm^{-1}K^{-1}$
τ	transport lifetime, s
Φ	interatomic force constants, harmonic: Jm^{-2}, anharmonic: Jm^{-3}
ω	frequency, rad/s
Subscripts	
α, β	Cartesian direction
k	unit cell atom label
l	unit cell label
scatter	phonon scattering mechanisms

This topical review will survey first principles (or ab initio) thermal transport as it relates to the Peierls-Boltzmann transport equation, from its origins to its applications, driving deeper understanding and predictions of κ and illuminating engineering pathways to manipulate κ in bulk and nanoscale systems.

Foundation of first principles thermal transport

Firstly, "first principles thermal transport" as it pertains to this topical review must be more specifically defined, unfortunately but necessarily limiting the scope: calculations of phonon κ based on interatomic forces from density functional theory (DFT) [9, 10] and solution of the Peierls-Boltzmann transport (PBT) equation [11–14]. Throughout this review, first principles Peierls-Boltzmann transport will be abbreviated fp-PBT.

Not so humble beginnings

Debye's theory of specific heat in dielectric solids [15, 16] went beyond simple noninteracting oscillators to energy being distributed among quantized normal modes of vibrations of the collective

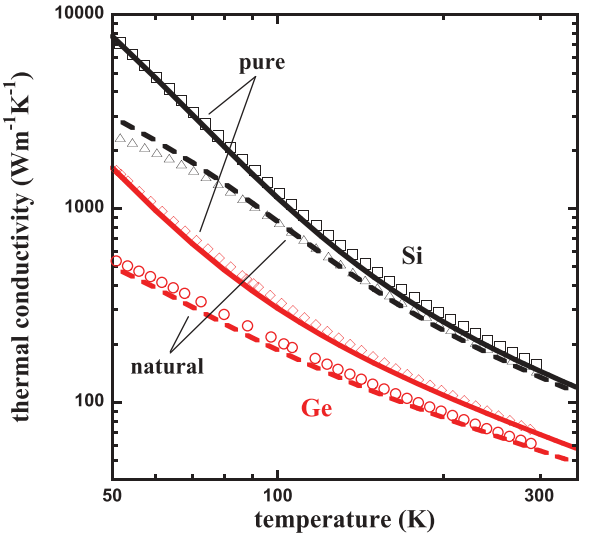

Figure 1. Calculated κ vs. temperature for Si (black curves) and Ge (red curves) with naturally occurring isotope concentrations (dashed curves) and isotopically enriched (solid curves). Corresponding measured data are given by red circles and diamonds [132] for Ge and black triangles and squares [133] for Si. This figure is adapted from Ward et al. [8] with permission.

set of atoms (phonons). As Debye and others argued [11, 17], to understand phenomena such as thermal expansion and finite intrinsic κ one must include anharmonic terms in the crystal potential, perturbation to the harmonic picture. Peierls extended Debye's ideas and Boltzmann's equation for dynamics of gases [18] to describe the transport properties of interacting phonons in a dielectric crystal [11, 12] given here as the Peierls-Boltzmann transport equation:

$$\vec{v}_{\vec{q}j} \cdot \vec{\nabla} T \left(\partial n_{\vec{q}j} / \partial T \right) = \left(\partial n_{\vec{q}j} / \partial t \right)_{\text{scatter}}, \tag{1}$$

where $\vec{v}_{\vec{q}j}$ is the velocity of a phonon with wavevector $\vec{q}$ in branch j, $\vec{\nabla} T$is a temperature gradient, $n_{\vec{q}j}$ is the nonequilibrium mode distribution, and the right-hand side is built from various phonon scattering mechanisms [13, 14]. Peierls also distinguished between Umklapp (U) processes (folding over of momentum) and Normal (N) processes (strict momentum conservation), the former providing the intrinsic resistance that degrades a thermal current. The PBT in Eq. (1) represents steady-state transport in a homogeneous system and is typically linearized; that is, $n_{\vec{q}j} = n^0_{\vec{q}j} + n^1_{\vec{q}j}$, where $n^0_{\vec{q}j}$ is the equilibrium Bose distribution and $n^1_{\vec{q}j}$ is the deviation from equilibrium linear in $\vec{\nabla} T$ [7]. A more general formulation of the PBT is space and time dependent [13, 19] and is more challenging to solve. Nonetheless, fp-PBT calculations have employed methods to determine temporally [20, 21] and spatially [21, 22] dependent phonon distributions in some systems.

In general the PBT is solved to determine phonon mode distributions and thus the transport lifetimes ($\tau_{\vec{q}j\alpha}$) that enter the equation for κ [13]:

$$\kappa_{\alpha\beta} = \sum_{\vec{q}j} C_{\vec{q}j} v_{\vec{q}j\alpha} v_{\vec{q}j\beta} \tau_{\vec{q}j\beta}, \tag{2}$$

where $C_{\vec{q}j}$ is the volume-normalized mode-specific heat and the Greek subscripts represent Cartesian directions. Unlike the commonly used relaxation time approximation (RTA), the $\tau_{\vec{q}j\alpha}$ defined here are constructed from the nonequilibrium distributions determined directly from full solution of Eq. (1) (iterative or otherwise) and carry directional dependence relative to the applied $\vec{\nabla} T$. (For cubic systems the conductivity tensor is diagonal and can be described by a single value, κ.) In practice, however, the solution of the PBT presents a significant challenge. Callaway wrote in 1959 [23]: "Although an exact

calculation of lattice thermal conductivity is possible in principle, lack of knowledge of crystal vibration spectra and of anharmonic forces in crystals and the difficulty of obtaining exact solutions of the Boltzmann equation are formidable barriers to progress." And Ziman elaborated in 1960 [13]: "The Boltzmann equation is so exceedingly complex that it seems hopeless to expect to generate a solution from it directly." Thus, many simplifications (e.g., the RTA) and models of varying complexity [23–26] have been employed, most with parameters adjusted to match measured κ data. Though they provide insights into lattice thermal transport of solids, these models lack predictive capabilities and can misrepresent the relative importance of competing scattering mechanisms.

With advances in high-performance computing and development of theoretical techniques such as density functional theory [9, 10], full solution of the fp-PBT with realistic interaction potentials is now possible. DFT describes many-body electron systems (e.g., crystalline solids) from functionals of space-dependent electron density. DFT has demonstrated significant success in describing many materials properties, and a number of convenient software packages are available; for example, ABINIT [27], Quantum Espresso [28], VASP [29], and WIEN2k [30]. We note that a dizzying array of implementations, approximations, and choices can be employed in DFT calculations. It is not in the scope of this topical review to cover such cases but to generally discuss application of DFT methods to thermal transport calculations.

Pre-History of fp-PBT: Necessary ingredients

Before embarking on discussion of fp-PBT results, three important ingredients will be highlighted: (1) harmonic interatomic force constants (IFCs; phonon dispersions), (2) third-order anharmonic IFCs (three-phonon interactions), and (3) a PBT solver (phonon lifetimes).

Phonon dispersions (frequencies, $\omega_{\vec{q}j}$, versus wavevector) are determined by building and diagonalizing the so-called dynamical matrix [13, 14, 16]

$$D_{\alpha\beta}^{kk'}(\vec{q}) = \frac{1}{\sqrt{m_k m_{k'}}} \sum_{l'} \Phi_{\alpha\beta}^{0k,l'k'} e^{i\vec{q}\cdot\vec{R}_{l'}} \tag{3}$$

for each $\vec{q}$. This is built from the atomic masses, m_k, and second derivatives of the DFT potential with respect to small atomic displacements, real-space harmonic IFCs ($\Phi_{\alpha\beta}^{0k,l'k'}$). Here, $\vec{R}_l$ is the lattice vector locating the lth unit cell and k labels the unit cell atom. Accurate lattice dynamical calculations are a critical building block for predictive thermal transport calculations. Full ab initio DFT phonon dispersions from lattice dynamics calculations were reported by Giannozzi et al. [31] in 1991 for Si, Ge, GaAs, AlAs, GaSb, and AlSb using density functional perturbation theory [32] and linear response methods. For all cases general agreement of calculated dispersions with measured data was obtained. Figure 2 illustrates this for the ionic rock salt alkali halide KBr. A good review of DFT lattice dynamical methods is given by Baroni et al. [32].

The next component in determining κ is a set of third-order anharmonic IFCs ($\Phi_{\alpha\beta\gamma}^{0k,l'k'l''k''}$) that give rise to couplings of three phonons. These IFCs enter the calculation of phonon transition rates for three-phonon scattering processes via Fermi's golden rule [13, 14] and build the right-hand side of Eq. (1). From 1995 through the mid-2000s, calculations of anharmonic line shifts, line broadenings, and lifetimes of zone center optic modes in elemental and III-V semiconductors from DFT linear response methods were presented [33–39] and obtained generally good agreement with measured data.

To determine κ from these IFCs two challenges remain: (1) determination of the phase space for phonon–phonon interactions and (2) solution of the PBT equation. We will discuss these in more detail below, but here it is worth noting the contributions of Omini and Sparavigna toward implementing a full solution of the PBT, beyond RTA methods. In their work, an iterative procedure for obtaining transport lifetimes from the linearized PBT was developed [40–42] with the zeroth-order term representing an RTA solution. We note that other PBT solution methods have also been developed [43].

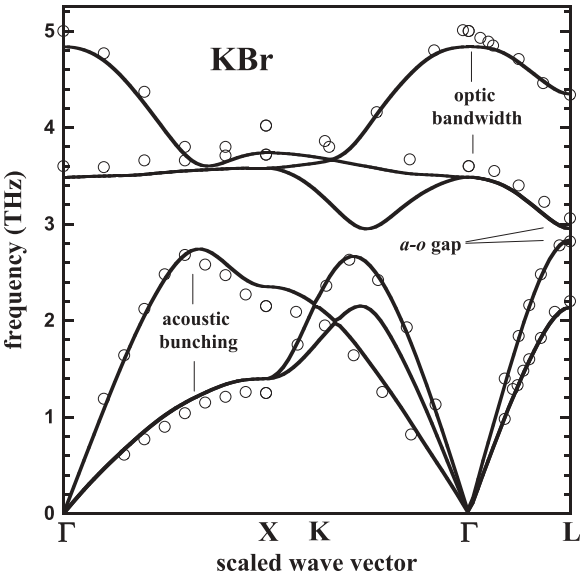

Figure 2. Calculated phonon dispersion for rock salt KBr (black curves) compared with measured data from neutron scattering [134]. Calculations were done using the Quantum Espresso package [28] within the generalized gradient approximation (Perdew-Burke-Ernzerhof) using Martins-Troullier norm-conserving pseudopotentials. The structure was determined by energy minimization (a = 6.440Å) using a 12 × 12 × 12 Monkhorst-Pack integration grid for electronic structure (100Ry planewave cutoff) and an 8 × 8 × 8 grid for harmonic IFC calculations.

A brief history of fp-PBT

With all of the necessary ingredients available, Broido et al. [7] reported in 2007 the first fully ab initio κ calculations using density functional perturbation theory for harmonic and anharmonic IFCs coupled with an iterative fp-PBT method. The agreement with measured κ data for isotopically purified Si and Ge, *without adjustable parameters*, was noteworthy. Nonetheless, fp-PBT got off to a slow start. In 2008, Esfarjani and Stokes [44] reported a method for extracting DFT anharmonic IFCs with a direct-space approach. In 2009, Ward et al. [8] reported the first calculations of ab initio κ with natural isotope abundances for Si, Ge, and diamond. Figure 1 here gives the Si and Ge calculations adapted from that work. Other early first principles calculations were published in 2010 and 2011: MgO at high temperature and pressure [45], Si-Ge alloys [46] and superlattices [47], Si nanowires [48], and half-Heuslers [49], a handful of papers over 5 years.

In the period 2012 to 2014 the number of materials examined via fp-PBT expanded, with an estimated publication count of approximately 20. Most notably, DFT thermal transport was coupled with high-profile experimental work (e.g., superlattices [50], thermoreflectance measurements [51], and neutron scattering [52]), predictions were made (e.g., ultrahigh κ of cubic BAs [53]; see Figure 3), and overall generally good agreement was attained with measured κ values of high-quality crystals from a number of research groups.

Beginning in 2014, publicly available software packages for calculating first principles anharmonic IFCs and solving the PBT became available, including ShengBTE [54], Phono3py [55], PhonTS [56], and ALAMODE [57], all with varying input and output parameters but with the same goal: predictive thermal transport capabilities. Now publications using fp-PBT are proliferating and are too numerous to count. We are gaining fundamental and technological insight into phonon transport of a variety of old and new systems, and advanced techniques are being developed to examine related properties with similar rigor (e.g., electron–phonon coupling [58]). The current challenge is to thoughtfully employ and further develop these technologies to find interesting materials and behaviors for both fundamental and applications-based research. The remaining sections will discuss

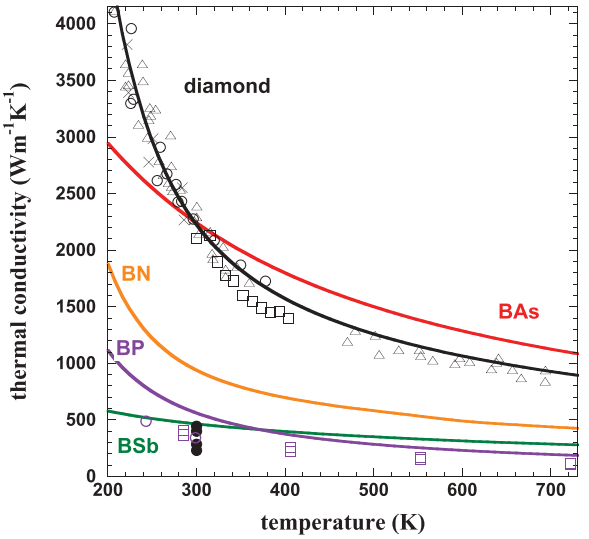

Figure 3. Calculated κ for cubic BN (orange), BP (purple), BAs (red), BSb (green), and diamond (black) with naturally occurring isotope concentrations. Available measured data are given for diamond: black squares [135], triangles [136], circles [137], crosses [138]; and BP: purple circles [139] and squares [140]. Solid black circles give commonly accepted room temperature κ values for high κ materials GaN, Al, AlN, Cu, and SiC. This figure is adapted from Lindsay et al. [53] with permission.

details of the physics and practical implementation of these methods, including unresolved issues and further challenges, with highlights from previous calculations interwoven throughout.

Application of fp-PBT: Concepts and highlights

In this section, highlights of recent fp-PBT work are presented with the goal of discussing important physical concepts and application challenges, including scattering phase space, N and U scattering, the RTA, lower dimensional systems, and mean free path spectroscopy.

Scattering phase space

Calculation of phonon–phonon scattering phase space [13, 59] has become an important tool for understanding the behavior of κ from material to material and under varying conditions (e.g., pressure) [8, 53, 59–65]. This phase space is determined by integrating over delta functions that represent the conservation of energy and crystal momentum conditions:

$$\omega_{\vec{q}j} \pm \omega_{\vec{q}'j'} = \omega_{\vec{q}''j''} \text{ and } \vec{q} \pm \vec{q}' = \vec{q}'' + \vec{G} \tag{4}$$

that enter scattering rate calculations and depend only on the phonon dispersions. This property is important because it measures the amount of scattering that a particular phonon mode can participate in, thus affecting its lifetime. $\vec{G} = 0$ for N processes and $\vec{G} \neq 0$ for Peierls' resistive U processes [11–13]. The integrals over the conservation conditions may also be weighted by the Bose factors of the phonons involved in each scattering process to give this phase space temperature dependence and provide further physical insights into thermal transport [55, 64]. Figure 4 gives the calculated phase space versus calculated κ for a number of materials to demonstrate its correlation with conductivity.

Accurate calculation of phase space and scattering rate integrals, and thus κ, requires careful consideration of the implementation of numerical methods (invariance constraints, grid densities, threshold parameters, smearing widths, etc.). Various Brillouin zone integration schemes have been

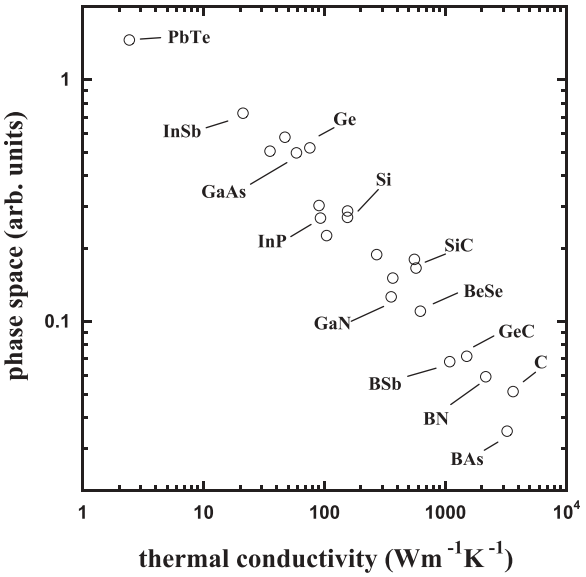

Figure 4. Calculated phase space vs. calculated κ for a set of isotopically pure cubic systems with a wide range of κ values. These phase space and κ values are determined from fp-PBT calculations and following methods of Lindsay and Broido [59].

employed in fp-PBT calculations, each maintaining a balance of efficiency and accuracy; for example, evenly spaced regularized Monkhorst-Pack meshes [54, 66] and uneven Gaussian quadrature rule methods as used in Lindsay and Broido [59] and Lindsay et al. [67]. Coupled with these integrations, conservation delta functions can be represented and integrated in a variety of ways, including direct root finding algorithms [59], tetrahedron method [55, 59, 68], and adaptive Gaussian smearing [54, 69]. Whatever the method employed, convergence of κ with respect to grid sampling densities and other internal parameters must be carefully considered.

The phase space dictated by the dispersion and conservation conditions governs the lifetimes for different phonon modes and has improved understanding of κ behavior in different materials. For instance, a large gap between acoustic and optic branches (*a*–*o* gap) in GaN was shown to limit acoustic phonon scattering and give relatively high κ, also leading to a prediction of large enhancement to room temperature κ with isotope enrichment of Ga [60]. Coupling the *a*–*o* gap with closely bunched acoustic branches led to the prediction of ultrahigh κ for an unlikely material, cubic BAs (~2,300 $Wm^{-1}K^{-1}$ at room temperature) [53], with κ values similar to that of diamond as shown in Figure 3. More recently, it has been shown that optic phonon bandwidth and dispersion give enhanced scattering and reduced κ values in a number of materials [61, 62].

N vs. U scattering, hydrodynamics, and the RTA

Another important consideration in κ calculations is whether the RTA is sufficient to describe nonequilibrium transport in a material. This has been shown to depend on the strength and number of resistive U processes compared to N processes, which play a critical role in redistributing phonons for thermal relaxation. Within the RTA N scattering is purely resistive and thus typically underestimates κ compared to a full PBT solution. Consequently, the RTA fails to properly describe κ in systems with generally weak U scattering, typically occurring in materials with high κ such as carbon-based materials (diamond [8], graphite [70], graphene [70, 71], and carbon nanotubes [72]). On the other hand, for lower κ systems, such as Si, Ge, and typical III-V compounds, the RTA falls within 5% of the full fp-PBT solution [67]. At low temperatures U scattering is frozen out and the RTA fails to describe intrinsic κ of any material. However, extrinsic scattering (e.g., grain

boundaries, point defects) becomes more important in this T regime, and first principles calculations become less reliable, requiring other extrinsic scattering models. We note that materials of interest for thermoelectrics applications likely are well characterized by the RTA [73].

Interestingly, some recent fp-PBT work in 2D materials predict the possibility of observing hydrodynamic phonon transport [74, 75] at temperatures well above the cryogenic conditions required for this observance in bulk materials [76]. These phenomena are not diffusive or ballistic in nature and derive from the collective macroscopic drift of phonons. This phenomenon depends critically on systems having weak U scattering.

Lower dimensional systems

Beyond bulk materials, first principles methods have been employed to examine κ in nanowires [22, 48, 73, 77], thin films [78, 79], carbon nanotubes [80], superlattices [47, 50], graphene [70, 71, 74, 75], and other 2D materials [65, 75, 81–87] with much success. A number of fp-PBT publications have explored the dependence of κ in graphene under various conditions (e.g., temperature, strain, size) with varying levels of success. Validation of first principles techniques is made difficult by large error bars for some measured graphene κ values and a significant range of reported values [88–92]. Outstanding questions seem to persist, including the following: What is the behavior of κ with increasing system size? Why do measured [88] and predicted [71] κ values disagree on the role of phonon–isotope scattering? Further investigations coupling fp-PBT and advanced experimental techniques to reduce measurement error may shed light on these issues.

Interestingly, a number of recent calculations have predicted significant in-plane anisotropy for another 2D system, single-layer black phosphorous [85–87]. The magnitudes of calculated κ differ (ranging from 30–110 $Wm^{-1}K^{-1}$ in the zigzag direction at room temperature), yet all predicted in-plane κ anisotropy ratios between 2.2 and 3.4. Figure 5 gives the calculated in-plane κ of phosphorene as functions of length and temperature, showing significant variation in in-plane transport. Subsequent measured data for thin-film black phosphorous samples also vary to some degree [93, 94] but verify the in-plane κ anisotropy. Similar behavior has been calculated for the high ZT thermoelectric material, bulk SnSe [95], and a new 2D material, borophene [96].

Calculations of κ for graphene's cousin, silicene, have demonstrated the importance of careful consideration of fp-PBT calculation details, including symmetry, testing of input parameters, and convergence. Varying values of calculated room temperature κ of silicene have been reported,

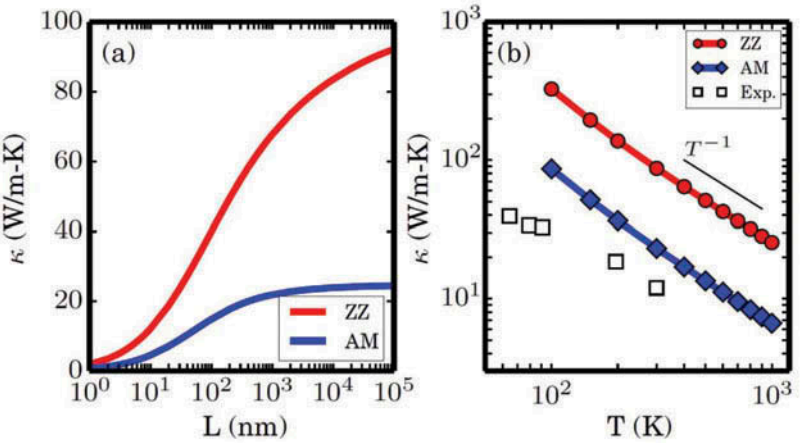

Figure 5. Calculated κ in zigzag (red) and armchair (blue) directions of phosphorene as a function of (a) sample length and (b) temperature. Black squares in (b) give measured κ data for bulk BP [141]. This figure is adapted from Zhu et al. [85] with permission.

particularly 9.4 $Wm^{-1}K^{-1}$ [97] and 36.2 $Wm^{-1}K^{-1}$ [98] (approximately four times larger) with the difference arising from the anharmonic IFCs. Another issue with κ calculations of silicene and other 2D materials is obtaining the correct low-frequency behavior of out-of-plane vibrational modes (ZA branch), which are sensitive to accurate calculation of harmonic IFCs and equilibrium invariance constraints. In unstrained graphene the ZA branch is quadratic, behavior also found in calculations for a number of 2D systems [83, 85, 96, 99]. However, some reported 2D dispersions give linear ZA branch behavior [65, 81, 86, 97, 98, 100], which can have significant consequences on the intrinsic phonon scattering and κ. It has been demonstrated recently that the ZA branch should be quadratic for arbitrary 2D systems [96].

Mean free path spectroscopy

New thermoreflectance-based measurement techniques [51, 101–103] now provide the unique opportunity to probe microscopic details of phonon thermal transport through mean free path spectroscopy: κ accumulation as a function of phonon mean free path. These methods go beyond bulk κ measurements to provide information of phonon mode contributions to the total κ and provide further benchmarks for fp-PBT. Thermoreflectance measurements and fp-PBT calculations have been compared for Si and other materials and will likely be extended to examine many more in the near future. Figure 6 gives calculated κ accumulation versus mean free path for Si compared to measured data.

Challenges that lie ahead

Thermal transport is an old and varied discipline in solid-state physics and engineering, yet application of first principles methods for predicting and characterizing κ is relatively new. In this section, discussion of the numerous challenges that lie ahead for application of fp-PBT to more complicated and realistic systems will be presented.

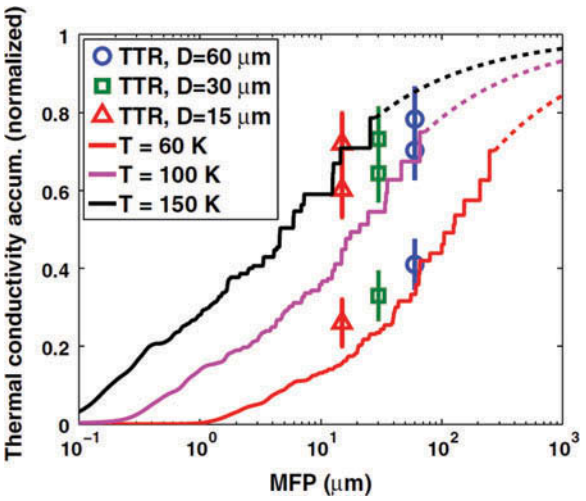

Figure 6. Calculated κ accumulation (curves) versus mean free path (MFP) for Si at T = 60K (red), T = 100K (pink), and T = 150K (blue). Symbols give measured data for varying pump beam diameter. This figure is adapted from Minnich et al. [101] with permission.

Inevitable extrinsic scattering in experiment

Since the development of fp-PBT methods and software and its initial benchmarking [7, 8], further validation of κ calculations by comparison with measured data is a significant obstacle. Characterization of intrinsic κ requires high-quality single-crystal samples, the growth of which is challenging especially for new materials. A further complication is that crystal quality characterization is difficult as typically types and concentrations of defects are not known from sample to sample. Thus, there are unique opportunities to develop rigorous first principles techniques and software to describe the various extrinsic phonon scattering mechanisms in solids and to collaborate with researchers dedicated to crystal growth and measurement techniques.

To describe extrinsic scattering mechanisms (e.g., boundary scattering in 2D materials [70, 71]) empirical models [13, 14] are often coupled with first principles methods. Phonon–isotope scattering [8, 104–106] is a rare case for which extrinsic scattering is on the same ground as intrinsic first principles methods (no input parameters), though one might argue that natural isotope concentrations are also an intrinsic property of a material. Regardless, the demonstrated agreement of ab initio κ calculations [8, 60] and measurements has required inclusion of phonon–isotope scattering from perturbation methods (see Figures 1 and 3). Recently, fp-PBT calculations have demonstrated that large enhancements to room-temperature κ with isotope purification is possible for some systems [60, 106], thus providing opportunities for increasing or manipulating κ with isotope modification. Further, encouraging first principles methods beyond simple mass perturbation are being developed to describe the effects of dilute point defects on κ, incorporating changes in bonding and local lattice distortions near defect sites [107].

In micro- and nanoelectronics, heat dissipation becomes a serious concern as power densities continue to decrease for size, cost, and function. Thus, cheap and efficient high-κ materials are of interest; however, these materials must make effective contact with the device and its packaging: interfacial thermal resistance may be just as important as bulk κ. Thus, another challenge for fp-PBT methods is to assimilate microscopic information into multiscale, multicomponent modeling efforts in a meaningful way. Such efforts may depend critically on seamless incorporation of atomistic behavior of bulk properties and interfaces (between materials and with the ambient environment) into macroscale models to develop an understanding of the overall transport behavior of devices.

Electrons and phonons

Perhaps the principal driver for the development and use of fp-PBT, and of especial importance for thermophysical engineering applications, is efficient thermoelectric materials. First principles methods have been employed to better understand intrinsically low κ in thermoelectric materials [49, 52, 61, 64, 73, 78, 108–111] and have coupled these methods with more traditional empirical models to incorporate the effects of extrinsic scattering mechanisms; for example, nanostructuring and alloying.

Mass perturbation scattering (similar to phonon–isotope scattering discussed above) in alloyed thermoelectric materials coupled with fp-PBT has also demonstrated surprising success when benchmarking against measured data for Si/Ge [46] and Mg_2Si/Mg_2Sn [73] alloys. Figure 7 demonstrates this, giving room-temperature calculated κ of Mg_2Si/Mg_2Sn alloys compared to measured data. These methods employed a virtual crystal approximation, mixing various properties of the pure systems based on alloy concentrations. The success is surprising given that alloys typically present large mass differences, not perturbative, and that IFC disorder is not considered. Calculations have also been employed to examine κ of PbTe/PbSe [108] and CdO/MgO [112] alloy systems.

Nanostructuring has become a popular route toward improving thermoelectric efficiency: scattering of phonons without degrading favorable electronic properties. To this end, significant work has demonstrated the capabilities for fp-PBT to describe κ in nanowires [22, 48, 73, 77] and superlattices [47, 50]. Figure 8 gives an example of fp-PBT κ in Si nanowire systems as a function of temperature compared to measured values of nanowires with varying diameters. These fp-PBT calculations were

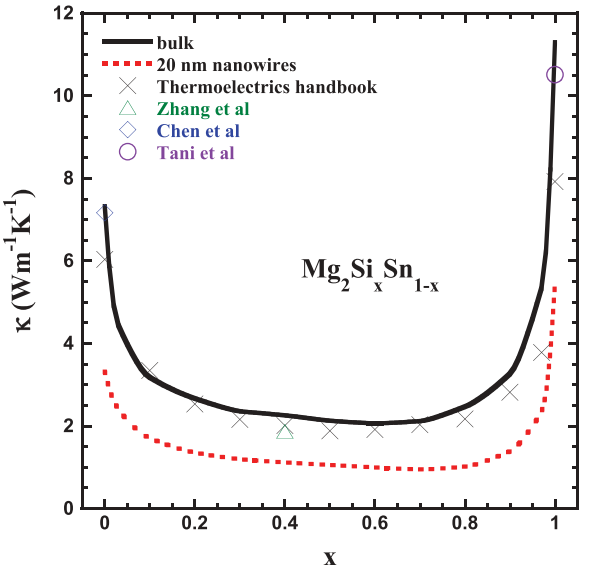

Figure 7. Room-temperature κ of $Mg_2Si_xSn_{1-x}$ as a function of *x* for both bulk materials (solid black curve) and 20-nm nanowires along [001] growth directions (dashed red curve), compared to measured data taken from Rowe's *Thermoelectrics Handbook* [142], Zhang et al. [143], Chen et al. [144], and Tani and Kido [145]. This figure is adapted with permission from Li et al. [73].

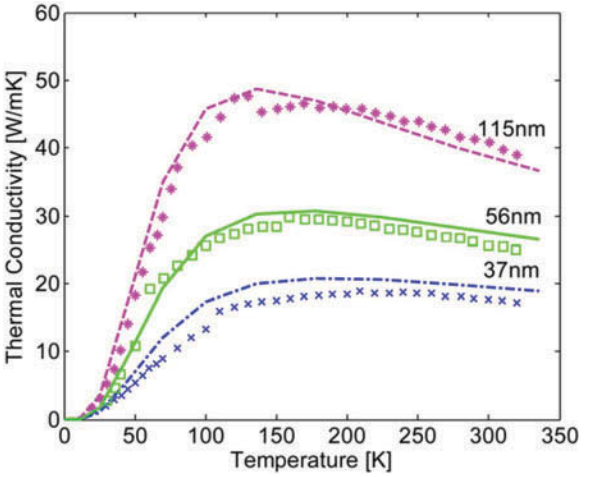

Figure 8. Calculated κ versus temperature (curves) of silicon nanowires for d = 37 nm (blue), 56 nm (green), and 115 nm (pink) compared to corresponding measured data (symbols) from Lie et al. [146]. This figure is adapted from Tian et al. [48] with permission.

coupled with an empirical boundary scattering model. In Lie et al. [22], fp-PBT calculations incorporating a real-space term in the PBT equation found higher κ values for Si nanowires than those from Tian et al. [48], likely due to an isotope scattering parameter employed in Tian et al. [48] that was 10 times too strong.

First principles methods to characterize electron–phonon coupling and its role in transport behaviors are also being developed [58] and applied to different systems; for example, highly doped semiconductors

[113] and metals [114, 115]. Challenges for describing coupled transport properties of materials include the need for high-density integration grids for accurate representation of the electronic and phononic structures.

DFT drawbacks relating to fp-PBT

First principles κ can suffer from issues that propagate from known drawbacks of standard DFT approximations and calculations. Two particular challenges are that DFT calculations typically (1) have volume prediction errors and (2) model zero-temperature ground states.

In general DFT does surprisingly well in equilibrium lattice constant prediction. Nonetheless, Haas et al. [116] compared measured and calculated lattice constants (a) of many cubic systems for a number of functionals showing that the local density approximation gives a ~1.3% too small and the generalized gradient approximation gives a ~1.1% too large. Despite these discrepancies, excellent agreement between calculated and measured values for phonon properties has been attained for many materials. However, for some systems, predicted a from energy minimization does not give the same agreement for phonon dispersions [60, 67, 117], particularly for optic phonons that provide important scattering channels for heat-carrying acoustic phonons. Underestimated a can give overestimated optic frequencies, thus resulting in calculated κ values that are too high. Note that simply using experimental a values often does not resolve this issue. Further, care should be taken in determining DFT input threshold and convergence parameters, as well as postprocessing translational invariance constraints [67], to accurately calculate ground-state structures and harmonic and anharmonic IFCs, because κ can depend sensitively on these. Jain and McGaughey [118] demonstrated differences in calculated κ of bulk Si from varying functionals and stressed the importance of strictly converging κ with respect to DFT criteria.

Temperature is a critically important parameter in determining κ, yet IFCs are typically determined from effectively zero-temperature ground-state systems. This approximation may be problematic for highly anharmonic systems whose atoms significantly deviate from equilibrium or for which thermal expansion may be important. Recently, significant theoretical efforts have been undertaken to describe the role of anharmonicity and temperature in systems that are otherwise predicted to be unstable (imaginary phonon modes) or for which typical fp-PBT methods fail [52, 109, 110, 119–124]. Such approaches include renormalization of harmonic phonon modes via anharmonic self-energies and ab initio molecular dynamics methods and have been used to more accurately predict finite-temperature equilibrium structures and phonon dispersions (e.g., bcc Zr [119, 120], palladium hydrides [122], and SrTiO3 [124]). Further, these methods have been applied to study phonon scattering and κ in PbTe [52, 109], InSb [123], Bi_2Te_3 [110], and SrTiO3 [124]. Further, higher order scattering beyond three-phonon processes may become important at higher temperature. The computational burden of calculating fourth-order scattering has prohibited its incorporation into fp-PBT methods. However, four-phonon scattering effects on κ of diamond, Si, and Ge have been recently explored via empirical potentials [125], perhaps foreshadowing the advent of such calculations from first principles.

Further future challenges

Beyond the complexities mentioned above, a number of other future challenges exist for fp-PBT. Application of first principles methods to complex crystal structures is challenging due to the many degrees of freedom. However, some κ calculations of fairly large unit cell systems have been done; for example, $YbFe_4Sb_{12}$ [64], Cu_2ZnSnS_4 [126], and Fe_2Ge_3 [127]. Further, in large unit cell systems scattering may become so strong that the phonon transport description may be more like that in nonperiodic amorphous materials, possibly requiring different descriptions of the behavior [128–130]. Rigorous high-throughput calculations of κ for giant material sets represents a daunting task for fp-PBT, yet better models may be developed, and insights obtained from fp-PBT calculations

may guide improved descriptors for use in high-throughput methods. Further, methods are being developed to more efficiently determine reduced IFC sets that maintain accurate descriptions of κ in materials [131]. As briefly discussed previously, more general fp-PBT methods are needed to describe thermal transport in systems for which spatial and temporal variance is important [20–22], such as in studies of hydrodynamic transport [74, 75]. Highly disordered systems (e.g., high entropy alloys) and soft matter (e.g., polymers) also represent significant challenges that require development of new tools and methods.

Conclusions

Significant new capabilities and tools for calculating, predicting, and understanding lattice thermal transport in a variety of systems have been recently developed. Building on the DFT formalism, fp-PBT equation methods are now becoming standard in applications to lattice thermal transport. Software packages for calculating first principles anharmonic properties and solving the PBT are newly available, and these techniques have been applied to many systems demonstrating generally good agreement with measured κ data in high quality samples.

This topical review discussed the foundations of fp-PBT and briefly considered important components of the calculation of thermal conductivity from first principles. Noteworthy highlights from previous research were presented, demonstrating the unique capabilities and challenges associated with these calculations. New understanding of phonon transport has been developed with the help of fp-PBT, and exciting predictions of phonon transport behavior have been made. Further advancement may give rise to engineered manipulation of phonon transport and better performing devices.

Acknowledgments

L.L. acknowledges support from the U. S. Department of Energy, Office of Science, Office of Basic Energy Sciences, Materials Sciences and Engineering Division and the National Energy Research Scientific Computing Center (NERSC), a DOE Office of Science User Facility supported by the Office of Science of the U.S. Department of Energy under Contract No. DE-AC02-05CH11231.

References

1. U.S. Department of Energy. Retrieved from http://energy.gov/eere/vehicles/vehicle-technologies-office-advanced-combustion-engines
2. G. Chen, *Nanoscale Energy Transport and Conversion: A Parallel Treatment of Electrons, Molecules, Phonons and Photons*, Oxford University Press, Oxford, 2005.
3. D.G. Cahill, P.V. Braun, G. Chen, D.R. Clarke, S. Fan, K.E. Goodson, P. Keblinski, W.P. King, G.D. Mahan, A. Majumdar, H.J. Maris, S.R. Phillpot, E. Pop, and L. Shi, Nanoscale Thermal Transport II, *Applied Physics Review*, Vol. 1, pp. 011305–11349, 2014.
4. Z. Tian, S. Lee, and G. Chen, Comprehensive Review of Heat Transfer in Thermoelectric Materials and Devices, *Annual Review of Heat Transfer*, Vol. 17, pp. 425–482, 2014.
5. D.R. Clarke and S.R. Phillpot, Thermal Barrier Coating Materials, *Materials Today*, Vol. 8, pp. 22–28, 2005.
6. P. Ball, Computer Engineering: Feeling the Heat, *Nature*, Vol. 492, pp. 174–175, 2012.
7. D.A. Broido, M. Malorny, G. Birner, N. Mingo, and D.A. Stewart, Intrinsic Lattice Thermal Conductivity of Semiconductors from First Principles, *Applied Physics Letters*, Vol. 91, pp. 231922–231925, 2007.
8. A. Ward, D.A. Broido, D.A. Stewart, and G. Deinzer, Ab Initio Theory of the Lattice Thermal Conductivity in Diamond, *Physical Review B*, Vol. 80, pp. 125203–125210, 2009.
9. P. Hohenberg and W. Kohn, Inhomogeneous Electron Gas, *Physical Review*, Vol. 136, pp. B864–B871, 1964.
10. W. Kohn and L.J. Sham, Self-Consistent Equations including Exchange and Correlation Effects, Physical Review, Vol. 140, pp. A1133–A1138, 1965.
11. R.E. Peierls, On the Kinetic Theory of Thermal Conduction in Crystals, *Annalen der Physik*, Vol. 3, pp. 1055–1100, 1929.
12. R.E. Peierls, *Quantum Theory of Solids*, Oxford University Press, London, 1955.
13. J.M. Ziman, *Electrons and Phonons*, Oxford University Press, London, p. 298, 1960.
14. G.P. Srivastava, *The Physics of Phonons*, Taylor & Francis Group, New York, 1990.

15. P. Debye, On the Theory of Specific Heats, *Annalen der Physik*, Vol. 344, pp. 789–839, 1912.
16. C. Kittel, *Introduction to Solid State Physics*, 7th ed., John Wiley & Sons, Inc., Hoboken, NJ, 1996.
17. P. Debye, Lectures on the Kinetic Theory of Matter and Electricity, in M. Planck et al., p. 43, B. G. Teubner, Leipzig, 1914.
18. L. Boltzmann, Further Studies on the Balance Among Gas Molecules, *Wiener Berichte*, Vol. 66, pp. 275–369, 1872.
19. N.W. Ashcroft and N.D. Mermin, *Solid State Physics*, Thomson Learning, Inc., Philadelphia, PA, 1976.
20. L. Chaput, Direct Solution to the Linearized Phonon Boltzmann Equation, *Physical Review Letters*, Vol. 110, pp. 265506–26510, 2013.
21. C.D. Landon and N.G. Hadjiconstantinou, Deviational Simulation of Phonon Transport in Graphene Ribbons with ab initio Scattering, *Journal of Applied Physics*, Vol. 116, pp. 163502–163512, 2014.
22. W. Li, N. Mingo, L. Lindsay, D.A. Broido, D.A. Stewart, and N.A. Katcho, Thermal Conductivity of Diamond Nanowires from First Principles, *Physical Review B*, Vol. 85, pp. 195436–195440, 2012.
23. J. Callaway, Model for Lattice Thermal Conductivity at Low Temperatures, *Physical Review*, Vol. 113, pp. 1046–1051, 1959.
24. P.G. Klemens, The Thermal Conductivity of Dielectric Solids at Low Temperatures (Theoretical), *Proceedings of the Royal Society of London, Series A*, Vol. 208, pp. 108–134, 1951.
25. P.B. Allen, Improved Callaway Model for Lattice Thermal Conductivity, *Physical Review B*, Vol. 88, pp. 144302–144306, 2013.
26. D.T. Morelli, J.P. Heremans, and G.A. Slack, Estimation of the Isotope Effect on the Lattice Thermal Conductivity of Group IV and Group III-V Semiconductors, *Physical Review B*, Vol. 66, pp. 195304–195312, 2002.
27. X. Gonze, J.-M. Beuken, R. Caracas, F. Detraux, M. Fuchs, G.-M. Rignanese, L. Sindic, M. Verstraete, G. Zerah, F. Jollet, M. Torrent, A. Roy, M. Mikami, Ph. Ghosez, J.-Y. Raty, and D.C. Allan, First-Principles Computation of Material Properties: the ABINIT Software Project, *Computational Materials Science*, Vol. 25, pp. 478–491, 2002.
28. P. Giannozzi, S. Baroni, N. Bonini, M. Calandra, R. Car, C. Cavazzoni, D. Ceresoli, G. L. Chiarotti, M. Cococcioni, I. Dabo, A. Dal Corso, S. de Gironcoli, S. Fabris, G. Fratesi, R. Gebauer, U. Gerstmann, C. Gougoussis, A. Kokalj, M. Lazzeri, L. Martin-Samos, N. Marzari, F. Mauri, R. Mazzarello, S. Paolini, A. Pasquarello, L. Paulatto, C. Sbraccia, S. Scandolo, G. Sclauzero, A.P. Seitsonen, A. Smogunov, P. Umari, and Re.M. Wentzcovitch, QUANTUM ESPRESSO: A Modular and Open-Source Software Project for Quantum Simulations of Materials, *Journal of Physics: Condensed Matter*, Vol. 21, pp. 395502–395521, 2009.
29. G. Kresse and J. Furthmüller, Efficiency of ab-initio Total Energy Calculations for Metals and Semiconductors Using a Plane-Wave Basis Set, *Computational Materials Science*, Vol. 6, pp. 15–49, 1996.
30. P. Blaha, K. Schwarz, G. Madsen, D. Kvasnicka, and J. Luitz, *WIEN2k, An Augmented Plane Wave + Local Orbitals Program for Calculating Crystal Properties*, Karlheinz Schwarz, Technische Universtiät Wien, Vienna, Austria, 2001.
31. P. Giannozzi, S. de Gironcoli, P. Pavone, and S. Baroni, Ab initio Calculation of Phonon Dispersions in Semiconductors, *Physical Review B*, Vol. 43, pp. 7231–7242, 1991.
32. S. Baroni, S. de Gironcoli, A. Dal Corso, and P. Giannozzi, Phonons and Related Crystal Properties from Density-Functional Perturbation Theory, *Reviews of Modern Physics*, Vol. 73, pp. 515–562, 2001.
33. A. Debernardi, S. Baroni, and E. Molinari, Anharmonic Phonon Lifetimes in Semiconductors from Density-Functional Perturbation Theory, *Physical Review Letters*, Vol. 75, pp. 1819–1823, 1995.
34. A. Debernardi, Phonon Linewidth in III-V Semiconductors from Density-Functional Perturbation Theory, *Physical Review B*, Vol. 57, pp. 12847–12858, 1998.
35. A. Debernardi, C. Ulrich, M. Cardona, and K. Syassen, Pressure Dependence of Raman Linewidth in Semiconductors, *Physica Status Solidi B*, Vol. 223, pp. 213–224, 2001.
36. G. Deinzer and D. Strauch, Raman Tensor Calculated from the 2*n*+1 Theorem in Density-Functional Theory, *Physical Review B*, Vol. 66, pp. 100301–100303, 2002.
37. G. Deinzer, G. Birner, and D. Strauch, Ab Initio Calculation of the Linewidth of Various Phonon Modes in Germanium and Silicon, *Physical Review B*, Vol. 67, pp. 144304–144309, 2003.
38. G. Deinzer, M. Schmitt, A.P. Mayer, and D. Strauch, Intrinsic Lifetimes and Anharmonic Frequency Shifts of Long-Wavelength Optical Phonons in Polar Crystals, *Physical Review B*, Vol. 69, pp. 014304–014310, 2004.
39. N. Bonini, M. Lazzeri, N. Marzari, and F. Mauri, Phonon Anharmonicities in Graphite and Graphene, *Physical Review Letters*, Vol. 99, pp. 176802–17805, 2007.
40. M. Omini and A. Sparavigna, An Iterative Approach to the Phonon Boltzmann Equation in the Theory of Thermal Conductivity, *Physica B: Condensed Matter*, Vol. 212, pp. 101–111, 1995.
41. M. Omini and A. Sparavigna, Beyond the Isotropic-Model Approximation in the Theory of Thermal Conductivity, *Physical Review B*, Vol. 53, pp. 9064–9073, 1996.
42. M. Omini and A. Sparavigna, Heat Transport in Dielectric Soldis with Diamond Structure, *Nuovo Cimento Della Societa Italina di Fisica D*, Vol. 19, pp. 1537, 1997.

43. G. Fugallo, M. Lazzeri, L. Paulatto, and F. Mauri, Ab initio Variational Approach for Evaluating Lattice Thermal Conductivity, *Physical Review B*, Vol. 88, pp. 045430–045438, 2013.
44. K. Esfarjani and H.T. Stokes, Method to Extract Anharmonic Force Constants from First Principles Calculations, *Physical Review B*, Vol. 77, pp. 144112–144118, 2008.
45. X. Tang and J. Dong, Lattice Thermal Conductivity of MgO at Conditions of Earth's Interior, *Proceedings of the National Academy of Sciences USA*, Vol. 107, pp. 4539–4543, 2010.
46. J. Garg, N. Bonini, B. Kozinsky, and N. Marzari, Role of Disorder and Anharmonicity in the Thermal Conductivity of Silicon–Germanium Alloys: A First-Principles Study, *Physical Review Letters*, Vol. 106, pp. 045901–04594, 2011.
47. J. Garg, N. Bonini, and N. Marzari, High Thermal Conductivity in Short-Period Superlattices, *Nano Letters*, Vol. 11, pp. 5135–5141, 2011.
48. Z. Tian, K. Esfarjani, J. Shiomi, A.S. Henry, and G. Chen, On the Importance of Optical Phonons to Thermal Conductivity in Nanostructures, *Applied Physics Letters*, Vol. 99, pp. 053122–053124, 2011.
49. J. Shiomi, K. Esfarjani, and G. Chen, Thermal Conductivity of Half-Heusler Compounds from First-Principles Calculations, *Physical Review B*, Vol. 84, pp. 104302–104310, 2011.
50. M.N. Luckyanova, J. Garg, K. Esfarjani, A. Jandl, M.T. Bulsara, A.J. Schmidt, A.J. Minnich, S. Chen, M.S. Dresselhaus, Z. Ren, E.A. Fitzgerald, and G. Chen, Coherent Phonon Heat Conduction in Superlattices, *Science*, Vol. 338, pp. 936–940, 2012.
51. K.T. Regner, D.P. Sellan, Z. Su, C.H. Amon, A.J.H. McGaughey, and J.A. Malen, Broadband Phonon Mean Free Path Contributions to Thermal Conductivity Measured Using Frequency Domain Thermoreflectance, *Nature Communications*, Vol. 4, pp. 1640–1646, 2013.
52. C.W. Li, O. Hellman, J. Ma, A.F. May, H.B. Cao, X. Chen, A.D. Christianson, G. Ehlers, D.J. Singh, B.C. Sales, and O. Delaire, Phonon Self-Energy and Origin of Anomalous Neutron Scattering Spectra in SnTe and PbTe Thermoelectrics, *Physical Review Letters*, Vol. 112, pp. 175501–175505, 2014.
53. L. Lindsay, D.A. Broido, and T.L. Reinecke, First-Principles Determination of Ultrahigh Thermal Conductivity of Boron Arsenide: A Competitor for Diamond? *Physical Review Letters*, Vol. 111, pp. 025901–025905, 2013.
54. W. Li, J. Carrete, N.A. Katcho, and N. Mingo, ShengBTE: A Solver of the Boltzmann Transport Equation for Phonons, *Computer Physics Communications*, Vol. 185, pp. 1747–1758, 2014.
55. A. Togo, L. Chaput, and I. Tanaka, Distributions of Phonon Lifetimes in Brillouin Zones, *Physical Review B*, Vol. 91, pp. 094306–094336, 2015.
56. A. Chernatynskiy and S.R. Phillpot, Phonon Transport Simulator (PhonTS), *Computational Physics Communications*, Vol. 192, pp. 196–203, 2015.
57. T. Tadano, Y. Gohda, and S. Tsuneyuki, Anharmonic Force Constants Extracted from First-Principles Molecular Dynamics: Applications to Heat Transfer Simulations, *Journal of Physics: Condensed Matter*, Vol. 26, pp. 225402–225413, 2014.
58. S. Poncé, E.R. Margine, C. Verdi, and F. Giustino, EPW: Electron–Phonon Coupling, Transport and Superconducting Properties Using Maximally Localized Wannier Functions, arXiv: 1604.03525, 2016.
59. L. Lindsay and D.A. Broido, Three-Phonon Phase Space and Lattice Thermal Conductivity in Semiconductors, *Journal of Physics: Condensed Matter*, Vol. 20, pp. 165209–165215, 2008.
60. L. Lindsay, D.A. Broido, and T.L. Reinecke, Thermal Conductivity and Large Isotope Effect in GaN from First Principles, *Physical Review Letters*, Vol. 109, pp. 095901–095905, 2012.
61. S. Lee, K. Esfarjani, T. Luo, J. Zhou, Z. Tian, and G. Chen, Resonant Bonding Leads to Low Lattice Thermal Conductivity, *Nature Communications*, Vol. 5, pp. 3525–3532, 2014.
62. S. Mukhopadhyay, L. Lindsay, and D.S. Parker, Optic Phonon Bandwidth and Lattice Thermal Conductivity: The Case of Li_2X (X=O, S, Se, Te), *Physical Review B*, Vol. 93, pp. 224301–224308, 2016.
63. X. Wu, J. Lee, V. Varshney, J.L. Wohlwend, A.K. Roy, and T. Luo, Thermal Conductivity of Wurtzite Zinc-Oxide from First-Principles Lattice Dynamics—A Comparative Study with Gallium Nitride, *Scientific Reports*, Vol. 6, pp. 22504–22513, 2016.
64. W. Li and N. Mingo, Ultralow Lattice Thermal Conductivity of the Fully Filled Skutterudite $YbFe_4Sb_{12}$ Due to the Flat Avoided-Crossing Filler Modes, *Physical Review B*, Vol. 91, pp. 144304–144309, 2015.
65. B. Peng, H. Zhang, H. Shao, Y. Xu, X. Zhang, and H. Zhu, Low Lattice Thermal Conductivity of Stanene, *Scientific Reports*, Vol. 6, pp. 20225–20234, 2016.
66. H.J. Monkhorst and J.D. Pack, Special Points for Brillouin-Zone Integrations, *Physical Review B*, Vol. 13, pp. 5188–5192, 1976.
67. L. Lindsay, D.A. Broido, and T.L. Reinecke, Ab initio Thermal Transport in Compound Semiconductors, *Physical Review B*, Vol. 87, pp. 165201–165215, 2013.
68. G. Lehmann and M. Taut, On the Numerical Calculation of the Density of States and Related Properties, *Physica Status Solidi B*, Vol. 54, pp. 469–476, 1972.
69. J.R. Yates, X. Wang, D. Vanderbilt, and I. Souza, Spectral and Fermi Surface Properties from Wannier Interpolation, *Physical Review B*, Vol. 75, pp. 195121–195131, 2007.

70. G. Fugallo, A. Cepellotti, L. Paulatto, M. Lazzeri, N. Marzari, and F. Mauri, Thermal Conductivity of Graphene and Graphite: Collective Excitations and Mean Free Paths, *Nano Letters*, Vol. 14, pp. 6109–6114, 2014.
71. L. Lindsay, W. Li, J. Carrete, N. Mingo, D.A. Broido, and T.L. Reinecke, Phonon Thermal Transport in Strained and Unstrained Graphene from First Principles, *Physical Review B*, Vol. 89, pp. 155426–155433, 2014.
72. L. Lindsay, D.A. Broido, and N. Mingo, Lattice Thermal Conductivity of Single-Walled Carbon Nanotubes: Beyond the Relaxation Time Approximation and Phonon–Phonon Scattering Selection Rules, *Physical Review B*, Vol. 80, pp. 125407–125413, 2009.
73. W. Li, L. Lindsay, D.A. Broido, D.A. Stewart, and N. Mingo, Thermal Conductivity of Bulk and Nanowire $Mg_2Si_xSn_{1-x}$ Alloys from First Principles, *Physcial Review B*, Vol. 86, pp. 174307–174314, 2012.
74. S. Lee, D.A. Broido, K. Esfarjani, and G. Chen, Hydrodynamic Phonon Transport in Suspended Graphene, *Nature Communications*, Vol. 6, pp. 6290–6299, 2015.
75. A. Cepelloti, G. Fugallo, L. Paulatto, M. Lazzeri, F. Mauri, and N. Marzari, Phonon Hydrodynamics in Two-Dimensional Materials, *Nature Communications*, Vol. 6, pp. 6400–6406, 2015.
76. H. Beck, P.F. Meier, and A. Thellung, Phonon Hydrodynamics in Solids, *Physica Status Solidi a*, Vol. 24, pp. 11–62, 1974.
77. W. Li and N. Mingo, Thermal Conductivity of Bulk and Nanowire InAs, AlN, and BeO Polymorphs from First Principles, *Journal of Applied Physics*, Vol. 114, pp. 183505–183508, 2013.
78. R. Guo, X. Wang, and B. Huang, Thermal Conductivity of Skudderudite $CoSb_3$ from First Principles: Substitution and Nanoengineering Effects, *Scientific Reports*, Vol. 5, pp. 7806–7814, 2015.
79. X. Wang and B. Huang, Computational Study of In-Plane Phonon Transport in Si Thin Films, *Scientific Reports*, Vol. 4, pp. 6399–6408, 2014.
80. S.-Y. Yue, T. Ouyang, and M. Hu, Diameter Dependence of Lattice Thermal Conductivity of Single-Walled Carbon Nanotubes: Study from ab Initio, *Scientific Reports*, Vol. 5, pp. 15440–15447, 2015.
81. X. Gu and R. Yang, First-Principles Prediction of Phononic Thermal Conductivity of Silicene: A Comparison with Graphene, *Journal of Applied Physics*, Vol. 117, pp. 025102–025116, 2015.
82. H. Liu, G. Qin, Y. Lin, and M. Hu, Disparate Strain Dependent Thermal Conductivity of Two-Dimensional Penta-Structures, *Nano Letters*, Vol. 16, pp. 3831–3842, 2016.
83. Y.D. Kuang, L. Lindsay, S.Q. Shi, and G.P. Zheng, Tensile Strains Give Rise to Strong Size Effects for Thermal Conductivities of Silicene, Germanene and Stanene, *Nanoscale*, Vol. 8, pp. 3760–3766, 2016.
84. W. Li, J. Carrete, and N. Mingo, Thermal Conductivity and Phonon Linewidths of Monolayer MoS_2 from First Principles, *Applied Physics Letters*, Vol. 103, pp. 253103–253106, 2013.
85. L. Zhu, G. Zhang, and B. Li, Coexistence of Size-Dependent and Size-Independent Thermal Conductivities in Phosporene, *Physical Review B*, Vol. 90, pp. 214302–214307, 2014.
86. A. Jain and A.J.H. McGaughey, Stongly Anisotropic In-Plane Thermal Transport in Single-Layer Black Phosphorene, *Scientific Reports*, Vol. 5, pp. 8501–8505, 2015.
87. G. Qin, Q.-B. Yan, Z. Qin, S.-Y. Yue, M. Hu, and G. Su, Anisotropic Intrinsic Lattice Thermal Conductivity of Phosphorene from First Principles, *Physical Chemistry Chemical Physics*, Vol. 17, pp. 4854–4857, 2015.
88. S. Chen, Q. Wu, C. Mishra, J. Kang, H. Zhang, K. Cho, W. Cai, A.A. Balandin, and R.S. Ruoff, Thermal Conductivity of Isotopically Modified Graphene, *Nature Materials*, 11, pp. 203–207, 2012.
89. A.A. Balandin, S. Ghosh, W.Z. Bao, I. Calizo, D. Teweldebrhan, F. Miao, and C.N. Lau, Superior Thermal Conductivity of Single-Layer Graphene, *Nano Letters*, Vol. 8, pp. 902–906, 2008.
90. S. Chen, A.L. Moore, W. Cai, J.W. Suk, J. An, C. Mishra, C. Amos, C.W. Magnuson, J. Kang, L. Shi, and R.S. Ruoff, Raman Measurements of Thermal Transport in Suspended Monolayer Graphene of Variable Sizes in Vacuum and Gaseous Environments, *ACS Nano*, Vol. 5, pp. 321–328, 2011.
91. X. Xu, L.F.C. Pereira, Y. Wang, J. Wu, K. Zhang, X. Zhao, S. Bae, C.T. Bui, R. Xie, J.T.L. Thong, B.H. Hong, K. P. Loh, D. Donadio, B. Li, and B özyilmaz, Length-Dependent Thermal Conductivity in Suspended Single-Layer Graphene, *Nature Communications*, Vol. 5, pp. 3689–3694, 2014.
92. I. Jo, M.T. Pettes, L. Lindsay, E. Ou, A. Weathers, A.L. Moore, Z. Yao, and L. Shi, Reexamination of Basal Plane Thermal Conductivity of Suspended Graphene Samples Measured by Eletro-Thermal Micro-Bridge Methods, *AIP Advances*, Vol. 5, pp. 053206–053217, 2015.
93. H. Jang, J.D. Wood, C.R. Ryder, M.C. Hersam, and D.G. Cahill, Anisotropic Thermal Conductivity of Exfoliated Black Phosphorus, *Advanced Materials*, Vol. 27, pp. 8017–8021, 2015.
94. Z. Luo, J. Maassen, Y. Deng, Y. Du, M.S. Lundstrom, P.D. Ye, and X. Xu, Anisotropic In-Plane Thermal Conductivity Observed in Few-Layer Black Phosphorus, *Nature Communications*, Vol. 6, pp. 8572–8579, 2015.
95. J. Carrete, N. Mingo, and S. Curtarolo, Low Thermal Conductivity and Triaxial Phononic Anisotropy of SnSe, *Applied Physics Letters*, Vol. 105, pp. 101907–101910, 2014.
96. J. Carrete, W. Li, L. Lindsay, D.A. Broido, L.J. Gallego, and N. Mingo, Physically Founded Phonon Dispersions of Few-Layer Materials and the Case of Borophene, *Materials Research Letters*, 2016. doi: 10.1080/21663831.2016.1174163
97. H. Xie, M. Hu, and H. Bao, Thermal Conductivity of Silicene from First-Principles, *Applied Physics Letters*, Vol. 104, pp. 131906–131909, 2014.

98. H. Xie, T. Ouyang, É. Germaneau, G. Qin, M. Hu, and H. Bao, Large Tunability of Lattice Thermal Conductivity of Monolayer Silicene via Mechanical Strain, *Physical Review B*, Vol. 93, pp. 075404–075413, 2016.
99. A. Molina-Sánchez and L. Wirtz, Phonons in Single-Layer and Few-Layer MoS_2 and WS_2, *Physical Review B*, Vol. 84, pp. 155413–155420, 2011.
100. X. Fan, W.T. Zheng, J.-L. Kuo, and D.J. Singh, Structural Stability of Single-Layer MoS_2 under Large Strain, *Journal of Physics: Condensed Matter*, Vol. 27, pp. 105401–105405, 2015.
101. A.J. Minnich, J.A. Johnson, A.J. Schmidt, K. Esfarjani, M.S. Dresselhaus, K.A. Nelson, and G. Chen, Thermal Conductivity Spectroscopy Technique to Measure Phonon Mean Free Paths, *Physical Review Letters*, Vol. 107, pp. 095901–095903, 2011.
102. Y. K. Koh and D. G. Cahill, Frequency Dependence of the Thermal Conductivity of Semiconductor Alloys, *Physical Review B*, vol 76, pp. 075207–075211, 2007.
103. J.A. Johnson, A.A. Maznev, J. Cuffe, J.K. Eliason, A.J. Minnich, T. Kehoe, C.M.S. Torres, G. Chen, and K.A. Nelson, Direct Measurement of Room-Temperature Nondiffusive Thermal Transport over Micron Distance in a Silicon Membrane, *Physical Review Letters*, Vol. 110, pp. 025901–025905, 2013.
104. S. Tamura, Isotope Scattering of Dispersive Phonons in Ge, *Physical Review B*, Vol. 27, pp. 858–866, 1983.
105. S. Tamura, Isotope Scattering of Large-Wave-Vector Phonons in GaAs and InSb: Deformation Dipole and Overlap-Shell Models, *Physical Review B*, Vol. 30, pp. 849–854, 1984.
106. L. Lindsay, D.A. Broido, and T.L. Reinecke, Phonon–Isotope Scattering and Thermal Conductivity in Materials with a Large Isotope Effect: A First-Principles Study, *Physical Review B*, Vol. 88, pp. 144306–144314, 2013.
107. N.A. Katcho, J. Carrete, W. Li, and N. Mingo, Effect of Nitrogen and Vacancy Defects on the Thermal Conductivity of Diamond: An ab initio Green's Function Approach, *Physical Review B*, Vol. 90, pp. 094117–094122, 2014.
108. Z. Tian, J. Garg, K. Esfarjani, T. Shiga, J. Shiomi, and G. Chen, Phonon Conduction in PbSe, PbTe, and $PbTe_{1-x}Se_x$ from First-Principles Calculations, *Physical Review B*, Vol. 85, pp. 184303–184309, 2012.
109. A.H. Romero, E.K.U. Gross, M.J. Verstraete, and O. Hellman, Thermal Conductivity in PbTe from First Principles, *Physical Review B*, Vol. 91, pp. 214310–214316, 2015.
110. O. Hellman and D.A. Broido, Phonon Thermal Transport in Bi_2Te_3 from First Principles, *Physical Review B*, Vol. 90, pp. 134309–134315, 2014.
111. J.M. Skelton, S.C. Parker, A. Togo, I. Tanaka, and A. Walsh, Thermal Physics of the Lead Chalcogenides PbS, PbSe, and PbTe from First Principles, *Physical Review B*, Vol. 89, pp. 205203–205212, 2014.
112. L. Lindsay and D.S. Parker, Calculated Transport Properties of CdO: Thermal Conductivity and Thermoelectric Power Factor, *Physical Review B*, Vol. 92, pp. 144301–144306, 2015.
113. B. Liao, B. Qiu, J. Zhou, S. Huberman, K. Esfarjani, and G. Chen, Significant Reduction of Lattice Thermal Conductivity by the Electron–Phonon Interaction in Silicon with High Carrier Concentrations: A First-Principles Study, *Physical Review Letters*, Vol. 114, pp. 115901–115906, 2015.
114. A. Jain and A.J.H. McGaughey, Thermal Transport by Phonons and Electrons in Aluminum, Silver, and Gold from First Principles, *Physical Review B*, Vol. 93, pp. 081206–081210, 2016.
115. Y. Wang, Z. Lu, and X. Ruan, First Principles Calculation of Lattice Thermal Conductivity of Metals Considering Phonon–Phonon and Phonon–Electron Scattering, *Journal of Applied Physics*, Vol. 119, pp. 225109–225118, 2016.
116. P. Haas, F. Tran, and P. Blaha, Calculation of the Lattice Constant of Solids with Semilocal Functionals, *Physical Review B*, Vol. 79, pp. 085104–085113, 2009.
117. T. Ruf, J. Serrano, M. Cardona, P. Pavone, M. Pabst, M. Krisch, M. D'Astuto, T. Suski, I. Grzegory, and M. Leszczynski, Phonon Dispersion Curves in Wurtzite-Structure GaN Determined by Inelastic X-ray Scattering, *Physical Review Letters*, Vol. 86, pp. 906–909, 2001.
118. A. Jain and A.J.H. McGaughey, Effect of Exchange-Correlation on First-Principles-Driven Lattice Thermal Conductivity Predictions of Crystalline Silicon, *Computational Materials Science*, Vol. 110, pp. 115–120, 2015.
119. P. Souvatzis, O. Eriksson, M.I. Katsnelson, and S.P. Rudin, Entropy Driven Stabilization of Energetically Unstable Crystal Structures Explained from First Principles Theory, *Physical Review Letters*, Vol. 100, pp. 095901–095904, 2008.
120. O. Hellman, I.A. Abrikosov, and S.I. Simak, Lattice Dynamics of Anharmonic Solids from First Principles, *Physical Review B*, Vol. 84, pp. 180301–180304, 2011.
121. O. Hellman and I.A. Abrikosov, Temperature-Dependent Effective Third-Order Interatomic Force Constants from First Principles, *Physical Review B*, Vol. 88, pp. 144301–144306, 2013.
122. I. Errea, M. Calandra, and F. Mauri, First-Principles Theory of Anharmonicity and the Inverse Isotope Effect in Superconducting Palladium–Hydride Compounds, *Physical Review Letters*, Vol. 111, pp. 177002–17706, 2013.
123. A.L. Miranda, B. Xu, O. Hellman, A.H. Romero, and M.J. Verstraete, Ab initio Calculation of the Thermal Conductivity of Indium Antimonide, *Semiconductor Science and Technology*, Vol. 29, pp. 124002–124006, 2014.
124. T. Tadano and S. Tsuneyuki, Self-Consistent Phonon Calculations of Lattice Dynamical Properties in Cubic $SrTiO_3$ with First-Principles Anharmonic Force Constants, *Physical Review B*, Vol. 92, pp. 054301–0543110, 2015.

125. T. Feng and X. Ruan, Quantum Mechanical Prediction of Four-Phonon Scattering Rates and Reduced Thermal Conductivity of Solids, *Physical Review B*, Vol. 93, pp. 045202–045211, 2016.
126. J.M. Skelton, A.J. Jackson, M. Dimitrievska, S.K. Wallace, and A. Walsh, Vibrational Spectra and Lattice Thermal Conductivity of Kesterite-Structured Cu_2ZnSnS_4 and $Cu_2ZnSnSe_4$, *APL Materials*, Vol. 3, pp. 041102–041107, 2015.
127. W. Li, J. Carrete, G.K.H. Madsen, and N. Mingo, Influence of the Optical–Acoustic Phonon Hybridization on Phonon Scattering and Thermal Conductivity, *Physical Review B*, Vol. 93, pp. 205203–205207, 2016.
128. P.B. Allen and J.L. Feldman, Thermal Conductivity of Disordered Harmonic Solids, *Physical Review B*, Vol. 48, pp. 12581–12588, 1993.
129. P.B. Allen, J.L. Feldman, J. Fabian, and F. Wooten, Diffusons, Locons and Propagons: Character of Atomic Vibrations in Amorphous Si, *Philosophical Magazine Part B*, Vol. 79, pp. 1715–1731, 1999.
130. H.R. Seyf and A. Henry, A Method for Distinguishing between Propagons, Diffusions, and Locons, *Journal of Applied Physics*, Vol. 120, pp. 025101–025107, 2016.
131. F. Zhou, W. Nielson, Y. Xia, and V. Ozoliņš, Lattice Anharmonicity and Thermal Conductivity from Compressive Sensing of First-Principles Calculations, *Physical Review Letters*, Vol. 113, pp. 185501–185505, 2014.
132. V.I. Ozhogin, A.V. Inyushkin, A.N. Taldenkov, A.V. Tikhomirov, G.E. Popov, E. Haller, and K. Itoh, Isotope Effect in the Thermal Conductivity of Germanium Single Crystals, *Journal of Experimental and Theoretical Physics Letters*, Vol. 63, pp. 490–494, 1996.
133. A.V. Inyushkin, A.N. Taldenkov, A.M. Gibin, A.V. Gusev, and H.-J. Pohl, On the Isotope Effect in Thermal Conductivity of Silicon, *Physica Status Solidi C*, Vol. 1, pp. 2995–2998, 2004.
134. A.D.B. Woods, B.N. Brockhouse, R.A. Cowley, and W. Cochran, Lattice Dynamics of Alkali Halide Crystals. II. Experimental Studies of KBr and NaI, *Physical Review*, Vol. 131, pp. 1025–1029, 1963.
135. D.G. Onn, A. Witek, Y.Z. Qiu, T.R. Anthony, and W.F. Banholzer, Some Aspects of the Thermal Conductivity of Isotopically Enriched Diamond Single Crystals, *Physical Review Letters*, Vol. 68, pp. 2806–2809, 1992.
136. J.R. Olson, R.O. Pohl, J.W. Vandersande, A. Zoltan, T.R. Anthony, and W.F. Banholzer, Thermal Conductivity of Diamond between 170 and 1200 K and the Isotope Effect, *Physical Review B*, Vol. 47, pp. 14850–14856, 1993.
137. L. Wei, P.K. Kuo, R.L. Thomas, T.R. Anthony, and W.F. Banholzer, Thermal Conductivity of Isotopically Modified Single Crystal Diamond, *Physical Review Letters*, Vol. 70, pp. 3764–3767, 1993.
138. R. Berman, R.R.W. Hudson, and M. Martinez, Nitrogen in Diamond: Evidence from Thermal Conductivity, *Journal of Physics C: Solid State Physics*, Vol. 8, pp. L430–L434, 1975.
139. G.A. Slack, Nonmetallic Crystals with High Thermal Conductivity, *Journal of Physics and Chemistry of Solids*, Vol. 34, pp. 321–335, 1973.
140. Y. Kumashiro, T. Mitsuhashi, S. Okaya, F. Muta, T. Koshiro, Y. Takahashi, and M. Mirabayashi, Thermal Conductivity of a Boron Phosphide Single-Crystal Wafer up to High Temperature, *Journal of Applied Physics*, Vol. 65, pp. 2147–2148, 1989.
141. G.A. Slack, Thermal Conductivity of Elements with Complex Lattices: B, P, S, *Physical Review*, Vol. 139, pp. A507–A515, 1965.
142. D.M. Rowe, *Thermoelectrics Handbook*, Taylor & Francis, New York, 2005.
143. Q. Zhang, J. He, T.J. Zhu, S.N. Zhang, X.B. Zhao, and T.M. Tritt, High Figures of Merit and Natural Nanostructures in $Mg_2Si_{0.4}Sn_{0.6}$ Based Thermoelectric Materials, *Applied Physics Letters*, Vol. 93, pp. 102109–102111, 2008.
144. H.Y. Chen, N. Savvides, T. Dasgupta, C. Stiewe, and E. Mueller, Electronic and Thermal Transport Properties of Mg_2Sn Crystals Containing Finely Dispersed Eutectic Structures, *Physica Status Solidi A*, Vol. 207, pp. 2523–2531, 2010.
145. J. Tani and H. Kido, Thermoelectric Properties of Bi-Doped Mg_2Si Semiconductors, *Physica B*, Vol. 364, pp. 218–224, 2005.
146. D. Li, Y. Wu, P. Kim, L. Shi, P. Yang, and A. Majumdar, Thermal Conductivity of Individual Silicon Nanowires, *Applied Physics Letters*, Vol. 83, pp. 2934–2936, 2003.